Myb−DNA Recognition: Role of Tryptophan Residues and Structural Changes of the Minimal DNA Binding Domain of c-Myb

Loussinée Zargarian,[‡] Véronique Le Tilly,[‡] Nadège Jamin,[§] Alain Chaffotte,[||] Odd S. Gabrielsen,[⊥] Flavio Toma,[#] and Bernard Alpert*,[‡]

Laboratoire de Biologie Physico-Chimique, UFR de Biochimie, Université Paris 7, 2, place Jussieu, 75251 Paris Cedex 05, France, CEA - INSTN, 91191 Gif sur Yvette Cedex, France, Institut Pasteur, Unité de Biochimie Cellulaire, 28, rue du Dr. Roux, 75724 Paris Cedex 15, France, Department of Biochemistry, University of Oslo, P.O. Box 1041 Blindern, 0316 Oslo, Norway, and Laboratoire de RMN, IRCOF UPRES-A 6014 CNRS, IFRMP N°23, Université de Rouen, 76821 Mont-Saint-Aignan Cedex, France

Received May 20, 1998; Revised Manuscript Received November 30, 1998

ABSTRACT: The Myb oncoprotein specifically binds DNA by a domain composed of three imperfect repeats, R_1, R_2, and R_3, each containing 3 tryptophans. The tryptophan fluorescence of the minimal binding domain, R_2R_3, of c-Myb was used to monitor structural flexibility changes occurring upon DNA binding to R_2R_3. The quenching of the Trp fluorescence by DNA titration shows that four out of the six tryptophans are involved in the formation of the specific R_2R_3−DNA complex and the environment of the tryptophan residues becomes more hydrophobic in the complex. The fluorescence intensity quenching of the tryptophans by binding of R_2R_3 to DNA is consistent with the decrease of the decay time: 1.46 ns for free R_2R_3 to 0.71 ns for the complexed protein. In the free R_2R_3, the six tryptophans are equally accessible to the iodide and acrylamide quenchers with a high collisional rate constant (4×10^9 and 3×10^9 M^{-1} s^{-1}, respectively), indicating that R_2R_3 in solution is very flexible. In the R_2R_3−DNA complex, no Trp fluorescence quenching is observed with iodide whereas all tryptophan residues remain accessible to acrylamide with a collisional rate constant slightly slower than that in the free state. These results indicate that (i) a protein structural change occurs and (ii) the R_2R_3 molecule keeps a high mobility in the complex.The complex formation presents a two-step kinetics: a fast step corresponding to the R_2R_3−DNA association (7×10^5 M^{-1} s^{-1}) and a slower one (0.004 s^{-1}), which should correspond to a structural reorganization of the protein including a reordering of the water molecules at the protein−DNA interface.

The c-myb proto-oncogene, which belongs to a large family of transcription factors found in a variety of species, is predominantly expressed in proliferating immature hematopoietic cells where it is thought to regulate cell proliferation and differentiation (*1*−*3*). The product of this gene, c-Myb, has been characterized as a nuclear phosphorylated multidomain protein of 75 kDa which is associated with chromatin. c-Myb is assumed to function as a regulator of gene expression by binding directly to Myb responsive elements in a variety of target genes (*4*−*8*). It has been found that c-Myb interacts specifically as a monomer with a PyAACG/TG target sequence (*9*−*11*).

Evolution has conserved in the different species the N-terminal part of the Myb proteins which corresponds to the DNA binding domain (DBD) of these transcription factors (*2*, *12*). This domain has a distinctive structure in that it consists of three homologous imperfect repeats (R_1, R_2, R_3) each containing 51−52 amino acids and has an unusually rich content of tryptophans. Each repeat contains in fact three conserved tryptophan residues spaced by 18−19 amino acids. Since the spacing of the rare amino acid tryptophan has been conserved by evolution, it has been suggested that this DBD is organized in a unique stereochemical arrangement in which the tryptophans might play an important structural and/or functional role (*13*, *14*). Both R_2 and R_3 are required for the sequence-specific binding (*15*, *16*), and these repeats bind to the target DNA sequences within the major groove of DNA (*17*). R_1 is dispensable for specific DNA binding (*18*); deletion of the R_1 repeat reduces the binding affinity by a factor 5.

Structure prediction by sequence homology suggested that each repeat contains three helices with the two C-terminal helices forming a helix-turn-helix (H-t-H) motif (*12*). On the basis of this model and the mutational effect on the binding affinity for the specific DNA sequence, c-Myb(R_2R_3) has been proposed to constitute the first example of a transcription factor binding DNA as a monomer by a double H-t-H motif (*18*) in which the third C-terminal helix of each repeat is the recognition helix.

NMR studies have reported the structure of R_2R_3 of c-Myb of different species and of B-Myb (*19*−*22*). As predicted the structure of mouse c-Myb(R_2R_3) presents 3 helices with the H-t-H arrangement of the two C-terminal helices. The isolated repeats have the same structure with three tryptophans participating in a hydrophobic cluster (*20*). In human/

[‡] Université Paris.
[§] CEA-INSTN.
[||] Institut Pasteur.
[⊥] University of Oslo.
[#] Université de Rouen.

10.1021/bi981199j CCC: $18.00
Published on Web 01/20/1999

chicken c-Myb(R_2R_3) (*19*) and B-Myb(R_2R_3) (*21*, *22*), the R_3 repeat was observed to also contain three helices; contrary to the mouse c-Myb the R_2 repeat of both of these proteins was found to be flexible and to miss the C-terminal recognition helix. In B-Myb(R_2R_3) the relative orientation of the two N-terminal helices in R_2 (*22*) differs considerably from the spatial arrangement of their counterparts in c-Myb-(R_2R_3) from mouse (*20*). It was suggested that, in the B-Myb and c-Myb proteins, the recognition helix of R_2 might be stabilized by binding to DNA (*19*, *21*, *22*).

Also in the bound state, a structural heterogeneity was observed between R_2R_3 of various Myb proteins. The mouse c-Myb(R_2R_3) in the complex was found to have the same structure as in the free state (*17*); on the other hand, the existence of two different bound forms was indicated by the NMR study of the human/chicken c-Myb(R_2R_3) complex (*23*). Other parallel investigations of various Myb proteins have provided further evidence that the Myb DNA binding domain can have variable conformational properties and stability which seem to be related to DNA binding recognition (*24*−*28*).

In this work we have used the fluorescence of the six tryptophans and their regular distribution throughout the entire R_2R_3 structure in an attempt to establish the possible role of these residues in Myb−DNA recognition and to probe structural flexibility changes caused by binding to DNA. The data presented in this paper provide a new insight into the Myb−DNA interaction.

MATERIALS AND METHODS

Samples. Protein c-Myb fragments, containing two repeated segments (R_2, R_3), were obtained following a procedure previously described (ref *23*, and references herein). The protein Myb fragment concentration was determined by using an extinction coefficient of 36 700 M^{-1} cm^{-1} at 280 nm. The 16-mer oligonucleotide, d(CCTAACGGTCTAA-TGG), and the complementary strand were synthesized on a 10 μM scale and purified by Eurogentec (Seraing, Belgium). The double-stranded DNA was obtained by heating a solution containing the two DNA strands at equal concentrations during 10 min at 85 °C and slowly cooling it down to 5 °C. Double-stranded DNA_{mim16} concentration was determined from the single-strand concentration using an extinction coefficient of 7830 M^{-1} cm^{-1} per base at 260 nm (*29*).

For all experiments, the DNA_{mim16} and protein Myb fragments were solubilized in a 50 mM sodium phosphate buffer, pH 7.0, with NaN_3 (0.05% w/w), 0.2 mM EDTA, and 2 mM β-mercaptoethanol to prevent oxidation of the free Cys residue which has been shown to play an important role in DNA binding (*30*).

Trp fluorescence spectra and decays of free and bound c-Myb R_2R_3 were collected using 2.5×10^{-7} M protein. Fluorescence spectra and decay times of the protein−DNA complex were measured at least 10 min after mixing the c-Myb R_2R_3 with the DNA_{mim16}. In a previous fluorescence study of the R_2R_3−DNA interaction, it was shown that both a specific complex (1:1 R_2R_3−DNA stoechiometry) and a nonspecific complex are formed depending on the ranges of the protein and DNA concentrations. The specific 1:1 R_2R_3−DNA complex was found to have a dissociation constant value, K_d, equal to 5.1×10^{-9} M, whereas the nonspecific complex had a $K_d = 2.7 \times 10^{-6}$ M (*23*). Thus the properties of the protein fluorescence in the corresponding Myb−DNA complex having a 1/1 stoichiometry were studied using a fixed 2.5×10^{-7} M protein concentration and various DNA concentrations up to 2.5×10^{-7} M in order to avoid the presence of unspecific complexes.

The kinetics of the protein−DNA binding, observed by the stopped-flow fluorescence technique, was carried out using a final protein concentration of 0.06×10^{-6} M with three DNA_{mim16} concentrations (0.25×10^{-6}, 0.5×10^{-6}, and 1.25×10^{-6} M). All data were collected at about 6 °C.

Decay Times, Spectra, and Trp Fluorescence-Quenching Measurements. Experimental fluorescence intensity decays were performed using time-correlated single photon counting with a laser/microchannel plate instrumentation. The excitation wavelength was 290 nm, and emission was detected at 345 nm, with a band-pass of 16 nm, at right angle after passing through a polarizer set at 54°7 (magic angle) to the vertical. The laser pulse duration was 1 ps, and fluorescence decay storage was collected in 2048 channels of 16 ps width. The instrumental response function was determined from the Rayleigh light scattered by the water at the excitation wavelength. Each decay curve typically contained 6×10^5 total counts and required 5−10 min to be collected. The function describing the fluorescence intensity decay, following δ-function excitation ($\approx$1 ps) is assumed to be of the form:

$$F(t) = \int_{\lambda_1}^{\lambda_2} \int_0^{\infty} f(\lambda,k) e^{-kt} dk d\lambda$$

where $k = 1/\tau$ and τ is the decay time, and λ is the emission wavelength in the λ_1−λ_2 range and t the time.

For distinct decay times, τ_i, the decay curve can be approximated by the summation:

$$F(t) = \sum \alpha_i e^{-t/\tau_i}$$

where α_i are the pre-exponential factors of each exponential function.

The relative intensity contribution, f_i, of each component to the total emission, F, is related to the pre-exponential factor, α_i, and the decay time, τ_i, by the relationship:

$$f_i = \frac{\alpha_i \tau_i}{\sum \alpha_i \tau_i}$$

so

$$\sum f_i = 1$$

Currently, Trp fluorescence-quenching experiments use an average fluorescence decay time determined by (*31*):

$$\tau = \sum_i f_i \tau_i$$

Only an average decay time value τ was extracted from the experimental fluorescence decay and used in the quenching experiments.

Steady-state fluorescence experiments were carried out on a SLM 8000. Trp fluorescence spectra were recorded between 300 and 440 nm by exciting the sample at 290 nm.

The band-passes used for excitation and emission were 2 and 8 nm, respectively. The emission wavelength increment was 2 nm with an acquisition time of 2 s. All measurements were carried out using 1 by 0.4 cm path lengths quartz cuvettes. Fluorescence emission spectra result from 12 accumulations, each corrected for buffer background contribution, consisting of the Raman peak, contaminant fluorescence, and dark counts. Spectra were corrected for the photomultiplier (Hamamatsu R928) and the monochromator (Jobin Yvon concave holographic grating) responses.

Trp fluorescence-quenching experiments were made by using iodide or acrylamide, two collisional quenchers both having an efficiency of γ equal to unity (*32*, *33*). For quenching by iodide (with concentrations ranging from 0 to 0.2 M), corrective amounts of NaCl were added to each sample in order to have the same ionic strength in all of the samples. Trp fluorescence intensities were obtained for each quenching experiment by integrating the Trp fluorescence spectra. For the experiments with acrylamide, to avoid correcting for its optical density, we measured fluorescence quenching on the averaged decay time values of the Trp fluorescence emission. Fluorescence-quenching data were analyzed according to the Stern−Volmer (*34*) and Lehrer (*33*) relations.

Dynamic quenching process, by acrylamide or iodide, is described by the classical Stern−Volmer relationship:

$$\frac{F_0}{F} = \frac{\tau_0}{\tau} = 1 + k_q \tau_0 [Q]$$

where F_0 and τ_0 and, F and τ are the intensities and the decay times in the absence and presence of quencher [Q] respectively; k_q is the bimolecular collisional rate constant between the quencher molecules and the Trp residues. The value of k_q is related to the environmental flexibility of the Trp fluorophores.

As R_2R_3 contains more than one tryptophan residue, the Lehrer plot (*33*) was used to determine the tryptophan accessible fraction to quencher molecules such as iodide or DNA:

$$\frac{F_0}{\Delta F} = \left[\sum_{i=1}^{n} \frac{f_i K_i [Q]}{1 + K_i [Q]}\right]^{-1}$$

where F_0 is the fluorescence intensity of the Trp residues before quenching, $\Delta F = F_0 - F$ is the fluorescence intensity decrease caused by a given quencher concentration [Q], $f_i = F_{0i}/F_0$ is the fractional contribution of fluorescence intensity F_{oi} of the i^{th} fluorophore to the total fluorescence F_o for the selected excitation and emission wavelengths, and K_i is the quenching constant of an individual accessible tryptophan residue.

If each accessible fluorophore to the quencher exhibits the same value of K, the equation becomes:

$$\frac{F_0}{\Delta F} = \frac{1}{f_a K [Q]} + \frac{1}{f_a}$$

where $f_a = \sum_{i=1}^{n} f_i$ is the maximum fraction of accessible fluorophores. From this equation, a plot of $F_0/\Delta F = f(1/[Q])$ yields a straight line whose extrapolation at $1/Q = 0$ gives the value of $1/f_a$ on the axis $F_0/\Delta F$.

If each accessible fluorophore has a different value of K, the Lehrer relationship can be written as:

$$\frac{F_0}{\Delta F} = \frac{1 + \sum_{i=1}^{n} K_i [Q] + \sum_{j,i,=1}^{n} K_i K_j [Q]^2 + ...}{\sum_{i=1}^{n} f_i K_i [Q](1 + \sum_{j=1}^{n} K_j [Q] + ...)}$$

where i and j correspond to the i^{th} and j^{th} fluorophores.

At low quencher concentrations, this relationship can be simplified as:

$$\frac{F_0}{\Delta F} = \frac{1}{\sum_{i=1}^{n} f_i K_i [Q]} + \frac{\sum_{i=1}^{n} K_i}{\sum_{i=1}^{n} K_i f_i}$$

where the inverse of $\sum_{i=1}^{n} K_i / \sum_{i=1}^{n} K_i f_i$ can be considered as an effective average of the maximum fraction of accessible fluorophores, $(f_a)_{eff}$, and $\sum_{i=1}^{n} K_i$ can be considered as an effective averaged quenching constant, $(K)_{eff}$.

Values of $(f_a)_{eff}$ and $(K)_{eff}$ associated with the accessible fluorophores are obtained from the extrapolated intercept on the $F_0/\Delta F$ axis of the Lehrer plot and the slope at low quencher concentrations, respectively.

Kinetic Measurements. Kinetics of interaction between R_2R_3 protein and DNA_{mim16} was performed in a SFM3 stopped-flow device (Biologic Claix, France) equipped with a fluorescence detection. The reservoirs, syringes, mixer, and flow cell were thermostated at 6 ± 1 °C by circulating water from a temperature-controlled water bath using a high flux pump. The excitation beam was generated by a 150 W xenon/Mercury lamp. The excitation wavelength was 295 nm (4 nm band-pass). The emitted light was collected at right angle through a 320 nm highpass filter. Protein and DNA solutions were separately introduced in two 20 mL syringes. Typically, 200 μL from each syringe was simultaneously injected in 25 ms in the flow cell and the recording was triggered at the end of the injection phase.

Determination of the first-order rate constant was performed according to nonlinear least-squares fitting, using the FigP software from Biosoft (Cambridge, UK). To evaluate the second-order rate constant of the interaction between R_2R_3 protein and DNA_{mim16}, we performed simulations of the kinetics using the adaptive Runge Kutta fifth-order method of the Personal Vissim program from Visual Solutions Inc.

RESULTS

Throughout all this work, the Trp fluorescence of R_2R_3 interacting with DNA was measured under the conditions corresponding to the stoechiometric 1:1 protein−DNA complex.

Spectra and Decay Times of Trp Fluorescence from R_2R_3 Both Free and Bound to DNA_{mim16}. The intensity of Trp fluorescence emission of R_2R_3 decreases by about 50% upon complex formation with specific DNA_{mim16} as shown in Figure 1 (left). A similar large fluorescence quenching was

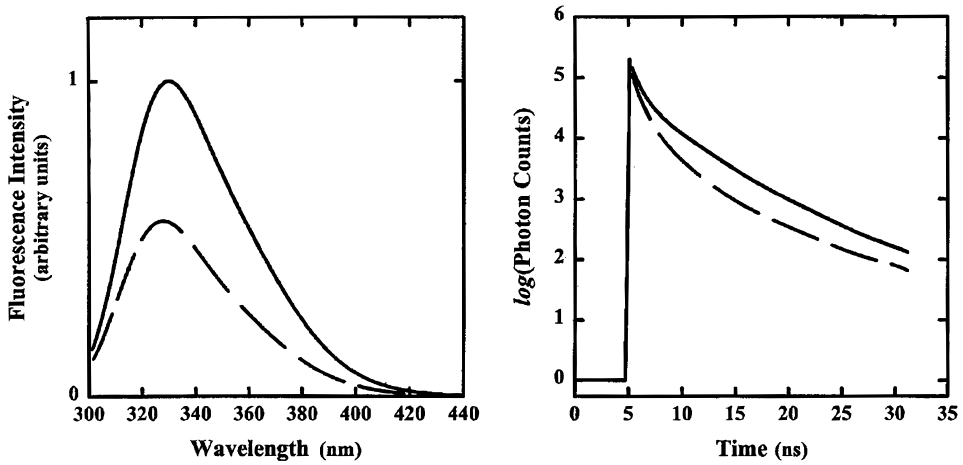

FIGURE 1: Left panel: Emission spectra of free R_2R_3 (—) and R_2R_3 bound to DNA_{mim16} (— — —). Right panel: Experimental Trp fluorescence intensity decay of free R_2R_3 (—) and of the R_2R_3—DNA complex (— — —). [R_2R_3] free and bound to DNA = 2.5×10^{-7} M, $\lambda_{excitation}$ = 290 nm.

previously reported in Trp fluorescence investigations of the R_2R_3 in the free and DNA-bound states (*24*). In addition, DNA binding of R_2R_3 is associated to the appearance of a blue shift (336 → 332 nm) of the fluorescence emission.

Trp fluorescence decay of both the free R_2R_3 and R_2R_3—DNA complex was also observed (Figure 1, right). The curves show that the decays are different for the two species, and cannot be approximated by single-exponential functions. By using the maximum entropy method (*35*), one can fit the Trp fluorescence decay of R_2R_3 with a good approximation by a sum of four exponential functions and the decay in the R_2R_3—DNA complex results from a sum of only three exponential functions. The relative intensity contributions of each component (f_i) were calculated from the decay time (τ_i) and the pre-exponential factor of each component (α_i). Then the average decay time values, τ_0, were obtained as described in Materials and Methods. The Trp fluorescence of free R_2R_3 exhibits an average decay time value of τ_0 = 1.46 ns and that of the specific R_2R_3—DNA complex an average decay time of τ_0 = 0.71 ns. This decrease of the fluorescence decay time in the Myb—DNA complex is consistent with the large decrease of the Trp fluorescence intensity upon DNA binding. These two latter effects are in agreement with the existence of contacts in the vicinity of the indole rings between the protein and the DNA.

Decay time and intensity variations of the Trp fluorescence were followed by titration of R_2R_3 with increasing amounts of DNA_{mim16} (Figure 2). The recorded fluorescence spectra (S) are a strict linear combination of the Trp fluorescence emission from the free R_2R_3 (S_f) and that of the specific R_2R_3—DNA complex (S_c):

$$S = \alpha S_f + (1 - \alpha)S_c \qquad \text{(a)}$$

Accordingly, fluorescence decay times (τ) also result from the same linear dependence of the Trp fluorescence decay times (τ_f and τ_c) of the two species:

$$\tau = \alpha\tau_f + (1 - \alpha)\tau_c \qquad \text{(b)}$$

The α values are taken as the fractions of the free protein, that is, $[R_2R_3]_{free}/[R_2R_3]_{total}$. Under the stoichiometric conditions (fixed protein concentration 2.5×10^{-7} M higher than the specific $K_d = 5.1 \times 10^{-9}$ M and lower than the unspecific

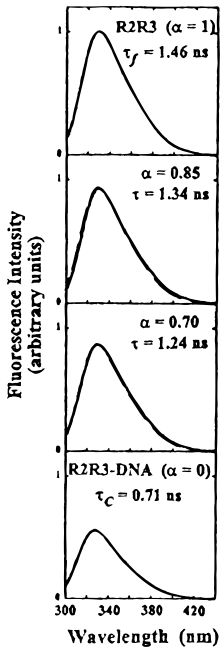

FIGURE 2: Experimental and calculated Trp fluorescence spectra of R_2R_3 (2.5×10^{-7} M) by titration with DNA_{mim16}: (—), experimental spectra; [1:1 R_2R_3—DNA complex] = $[DNA]_{total}$; from top to bottom [DNA] = (0, 3.7×10^{-8}, 7.3×10^{-8}, 2.5×10^{-7} M); $[R_2R_3]_{free} = [R_2R_3]_{total} - [DNA]_{total}$; (— — —) calculated spectra. Spectra were computed by using the linear combination of the α fraction of free R_2R_3 (f) with the $(1 - \alpha)$ fraction of the R_2R_3—DNA complex (c): $S = \alpha S_f + (1 - \alpha)S_c$ and $\tau = \alpha\tau_f + (1 - \alpha)\tau_c$ where $\alpha = [R_2R_3]_{free}/[R_2R_3]_{total}$.

$K_d = 2.7 \times 10^{-6}$ M), [1:1 complex] = $[DNA]_{total}$ and $[R_2R_3]_{free} = [R_2R_3]_{total} - [DNA]_{total}$.

Experimental and calculated results being rigorously identical in the two relations (a) and (b), the experimental Trp fluorescence emission of each sample is directly correlated to the number of free R_2R_3 proteins and to that of R_2R_3—DNA complexes in the solution (Figure 2). This shows that two independent species contribute to the total fluorescence observed: one corresponds to the free R_2R_3 protein (f) in solution and the other to the R_2R_3 protein complexed to DNA (c). These data, which show that only the specific 1:1 protein—DNA complex is formed, are in agreement with previous polarization studies on fluorescein-labeled DNA

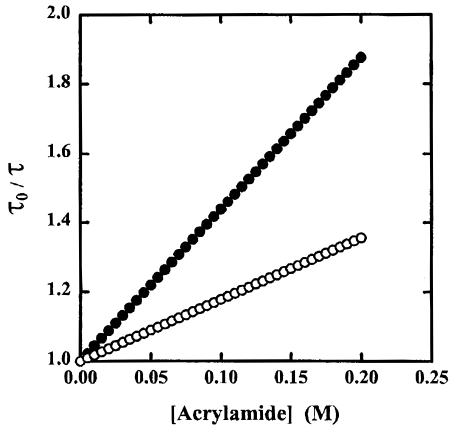

FIGURE 3: Stern−Volmer plots of the Trp fluorescence quenching of R_2R_3 by acrylamide: free R_2R_3 (●) and R_2R_3−DNA complex (○). τ_0 and τ are the averaged Trp fluorescence decay times, without and with acrylamide, respectively. The different slopes ($k_q\tau_0$) of the two species show the change of their k_q values: $\lambda_{excitation}$ = 290 nm; [R_2R_3] free and bound to DNA = 2.5×10^{-7} M.

(*23*). Each species is characterized by a distinct fluorescence decay time and by a specific fluorescence spectrum that correspond to Trp residues, for both the free R_2R_3 and the specific 1:1 R_2R_3−DNA complex, in different environments. In the specific protein−DNA complex the blue shift of the indole emission suggests, in addition, a shielding of its Trp side chains in a more hydrophobic environment than those of free R_2R_3.

In addition, these results show that the dissociation time of the protein−DNA complex is much longer than the times of the Trp fluorescence emissions.

R_2R_3 Structural Flexibility Changes upon DNA Binding. Whatever the location of Trp residues inside the protein, neutral acrylamide molecules are known to reach the Trp fluorophores in the protein matrix and quench their fluorescence emission. Accordingly, the Trp fluorescence of the free and DNA-bound R_2R_3 were found to be quenched by acrylamide.

The Stern−Volmer relationship was determined:

$$\tau_0/\tau = 1 + k_q\tau_0[Q]$$

where τ_0 and τ are the mean decay times of the Trp fluorescence measured respectively in the absence and in the presence of acrylamide quencher; k_q is the bimolecular kinetic constant of the Trp-acrylamide quenching and [Q] the concentration of acrylamide in solution.

Figure 3 exhibits the increase of the ratio τ_0/τ as a function of the acrylamide concentration. The slopes ($k_q \times \tau_0$) of the straight lines give the values of the collisional kinetic constant of $k_q = 2.5 \times 10^9$ M^{-1} s^{-1} for the protein−DNA complex and $k_q = 3 \times 10^9$ M^{-1} s^{-1} for the free protein.

Thus, the random migration of the quencher molecules in the vicinity of Trp residues is slightly slower in the R_2R_3−DNA complex than for R_2R_3 alone in solution indicating that the contact region between the protein and DNA molecules has an influence on the R_2R_3 protein flexibility.

Tryptophan Accessibility in Free and DNA-Bound R_2R_3. To explore in more detail the different environments of the Trp residues in the free and bound form, we studied their accessibility by the collisional quenching of the Trp fluorescence with iodide (*32*, *33*). Iodide bears one negative charge and may thus be supposed to mimic the charge effect of the DNA fragment when it interacts with Trp regions of the protein. If Trp residues are located in a positively charged region or are partially exposed to the solvent, the increase of the iodide concentration should result in a decrease of the Trp fluorescence intensity.

Figure 4 (left panel) displays the Trp emission spectra in the presence of different iodide concentrations (up to 0.20 M) for the free protein in solution. For a protein such as R_2R_3 which contains six Trp residues, the presence or the absence of charges in the surroundings of the Trp side chain is reasonably expected to influence the accessibility to iodide. Thus, to determine the number of Trp residues accessible to iodide, we have analyzed the Trp fluorescence-quenching data using the Lehrer relationship (see Methods):

$$\frac{F_0}{\Delta F} = \frac{1}{f_a K[Q]} + \frac{1}{f_a}$$

where [Q] is the iodide concentration. Analysis of the plot (Figure 4, right panel) gives a value for the fraction of accessible Trp residues, f_a, equal to 1 and the quenching Lehrer constant, K, equal to 5.8 M^{-1}. These values show that the six Trp residues, distributed in the protein fragment R_2R_3, are all quenched by iodide with the same quenching constant. This result indicates also that each Trp residue is located in an environment devoid of strong negative charges since this would otherwise repel the negatively charged iodide.

Since the Trp quenching by iodide arises from a collisional process, the Lehrer constant K is associated to the collisional quenching rate constant ($k_q = K/\tau_0$). Its value, $k_q = 4 \times 10^9$ M^{-1} s^{-1}, is of the same order of magnitude as that of free indole quenched in solution (6.4×10^9 M^{-1} s^{-1}) (*36*) and is consistent with Trp residues largely exposed to the solvent.

Accessibility of Trp residues in the R_2R_3−DNA complex was also performed by iodide quenching. In contrast to the free protein, no effect on Trp fluorescence intensity has been observed for bound R_2R_3, indicating that the Trp fluorophores are not accessible to the negatively charged iodide quencher.

Number of Interacting Trp Residues with DNA. To determine the number of tryptophan residues involved in the interaction of R_2R_3 with DNA_{mim16}, we collected Trp fluorescence intensities of the R_2R_3 protein (2.5×10^{-7} M) in the presence of variable DNA_{mim16} concentrations ($<2.5 \times 10^{-7}$ M). Under these conditions, only the specific 1:1 Myb−DNA complex is formed (cf. Materials and Methods, ref *23*). The Lehrer plot, $F_0/\Delta F = f(1/[DNA])$ (Figure 5), yields an accessible fraction, $(f_a)_{eff}$, equal to 0.67 by extrapolating to $1/[DNA]_{total} = 0$. Thus, about 67% of the Trp fluorescence intensity is quenched and 33% is not affected by DNA. Assuming that each Trp residue has the same fluorescence quantum yield, the value, $(f_a)_{eff} = 0.67$, shows that four out of the six Trp residues are involved in the association with DNA in the specific R_2R_3−DNA complex.

For higher protein and DNA concentrations (both ranging from 2.5×10^{-7} to 3×10^{-6} M), the observed Trp fluorescence intensities result from both the fluorescence of the specific complex and the fluorescence of the nonspecific complexes (see Materials and Methods) with 1:1, 2:1, 3:1, and 4:1 R_2R_3−DNA stoechiometries (data not shown,

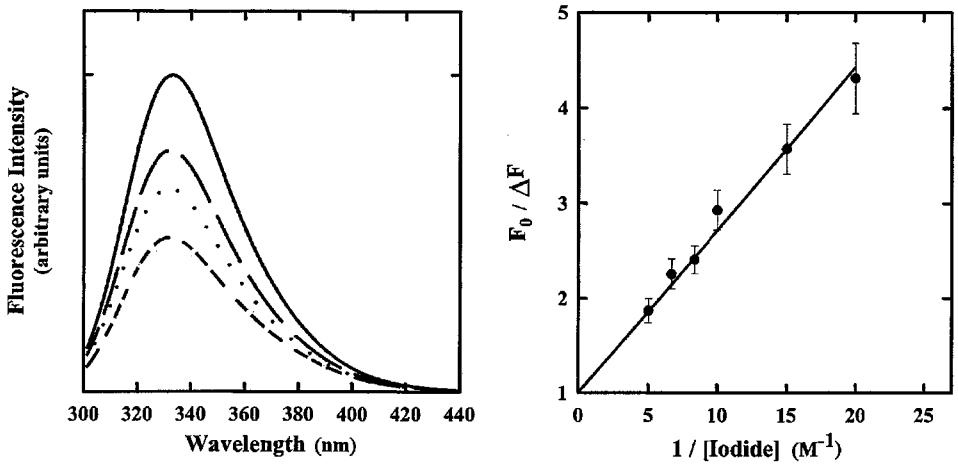

FIGURE 4: Left panel: Emission spectra of R_2R_3 (2.5×10^{-7} M) as a function of iodide concentrations: (—) R_2R_3 without iodide; (− − −) R_2R_3 with 0.05 M; (•••) 0.1 M; and (---) 0.2 M iodide concentrations. Right panel: Lehrer plot of the Trp fluorescence quenching of R_2R_3 by iodide: F_0 = Trp fluorescence intensity of free R_2R_3; F = Trp fluorescence intensity of R_2R_3 in the presence of iodide; $\Delta F = F_0 - F$, decrease of Trp fluorescence intensity of R_2R_3 induced by Trp−iodide collisions. Corrective amounts of NaCl were added in order to have the same ionic strength in each sample.

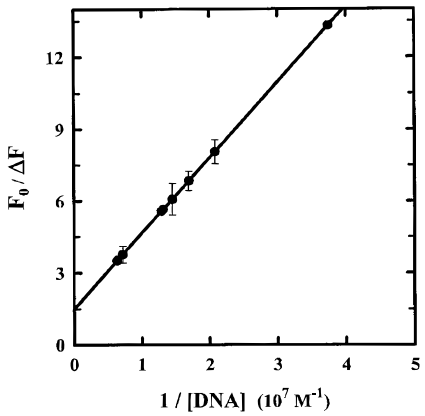

FIGURE 5: Lehrer plot of the Trp fluorescence quenching of R_2R_3 (2.5×10^{-7} M) by DNA: F_0, Trp fluorescence intensity of free R_2R_3; F = Trp fluorescence intensity of R_2R_3 in the presence of DNA; $\Delta F = F_0 - F$, Trp fluorescence intensity decrease in R_2R_3 at various DNA concentrations; DNA concentration range, 2.7×10^{-8}−1.4×10^{-7} M.

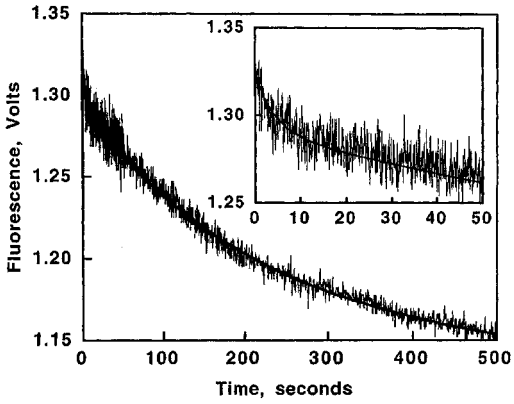

FIGURE 6: Kinetics of R_2R_3−DNA complex formation: 200 μL of 0.12 μM R_2R_3 were mixed with 200 μL of 0.5 μM DNA (see Experimental Section), and the fluorescence change (excitation at 295 nm) was recorded as a function of time. The kinetics trace results from pasting three successive regions. The first region (0−50 s) contains 1001 data points recorded with a sampling period of 50 ms and a time constant of 50 ms. The second region (50.2−200 s) contains 750 data points recorded with a sampling period of 200 ms and a time constant of 100 ms. The third region (200.5−500 s) contains 600 data points recorded with a sampling period of 500 ms and a time constant of 500 ms. The solid thick line corresponds to the best simulation using an adaptative Rung Kutta fifth-order numerical integrator. The RMS value was 4.36×10^{-5} V.

Zargarian, Thesis, 1997). The number of Trp residues involved in the protein−DNA contacts of these complexes was not studied and could be protein−DNA concentration-dependent.

Significantly, whereas all of the Trp residues in free R_2R_3 are easily accessible to iodide, as shown above, none of them are quenched by iodide anions in the DNA−R_2R_3 specific complex; however they are all quenched by acrylamide in the complex. Structural modifications around the Trp side chains are likely to occur in bound R_2R_3 and to prevent iodide/Trp collisions whereas they have no influence on acrylamide/Trp collisions. This result correlates well with both the blue shift and the 50% quenching observed by binding of R_2R_3 to DNA in 1/1 stoichiometric conditions.

Kinetics of R_2R_3 Structural Recognition upon DNA Binding. To further characterize the R_2R_3 recognition by DNA, we performed kinetic experiments by a stopped-flow device using fluorescence detection. As shown in Figure 6, mixing R_2R_3 at 0.06 μM with DNA at 0.25 μM results in a quenching of the intrinsic tryptophan fluorescence. Under the conditions of mixing used (25 ms), the kinetics process is clearly multiphasic. The fast initial decrease of fluorescence has been found to be dependent on DNA concentration (up to 1.25 μM DNA; data not shown) and to be related to the bimolecular process of the R_2R_3−DNA association. This step is followed by a slow decrease of Trp fluorescence which reaches a plateau after 500 s. This slow phase is independent of DNA concentration (data not shown) and is satisfactorily fitted by a single exponential yielding a rate constant value of 0.004 s^{-1}. To extract the kinetic parameters of the fast initial phase, we performed numerical simulations of the overall kinetics using the following 2-step model:

$$\text{P} + \text{DNA} \xrightarrow{k_1} \text{P-DNA} \xrightarrow{k_2} \text{P}'\text{-DNA}$$

Since the concentrations of free protein and DNA used in the kinetic experiments were at least 10 times higher than

the equilibrium dissociation constant of the protein−DNA 1:1 complex (5.1×10^{-9} M) (*23*), we considered the association step as a pseudo-irreversible process. The rate constant k_2 is fixed at 0.004 s^{-1}, as deduced from the fit of the isolated slow phase of the experimental kinetics. On the basis of the RMS value, the best simulation (see Figure 6) corresponds to a k_1 value of 7×10^5 M^{-1} s^{-1} for the fast step of Myb−DNA interaction. This value falls in the range of bimolecular rate constants for the association processes between medium-sized macromolecules (*37*).

DISCUSSION

This work reveals new features of the structural and dynamical behavior of the c-Myb minimal binding domain R_2R_3 and the relationship to DNA recognition.

Overall, the fluorescence data reported here indicate that the free R_2R_3 in aqueous solution is characterized by structural fluctuations in various parts of the domain. In fact, all of the Trp residues in R_2R_3 appear to be accessible to fluorescence inhibitors as different as iodide and acrylamide. The Lehrer plots with both quenchers show that the side chains of the six Trp are exposed to the solvent. The average collisional rate constant of iodide quenching (4.9×10^9 M^{-1} s^{-1}), observed for the Trp residues, has the same order of magnitude as the collisional rate measured for the free indole in aqueous solution (6.4×10^9 M^{-1} s^{-1}), which hints at the accessibility of the Trp fluorophores on a dynamical basis. Nevertheless, ionic interactions between iodide ions and positively charged basic residues, possibly in a region close to the Trp indoles, can also contribute to the high value of the collisional rate constant observed. In fact, the influence of electrostatic interactions on iodide quenching has already been demonstrated (*33*).

In contrast to iodide, no electrostatic effect is expected to contribute to Trp fluorescence quenching by the electrically neutral acrylamide molecule. Actually, the collisional rate constant measured with acrylamide (3×10^9 M^{-1} s^{-1}) is close to that found for a Trp residue in a random coil polypeptide (4×10^9 M^{-1} s^{-1}) (*38*), bringing further evidence for the large solvent exposure of the Trp side chains in R_2R_3. The Trp side chains can either be accessible by their position at the surface of the protein structure or alternatively become accessible, if buried in hydrophobic regions of the structure, via large internal motions. Both situations could occur for the 6 Trp residues in R_2R_3. NMR studies of mouse c-Myb-(R_2R_3) indicated that R_2 and R_3 folded independently, each forming a cluster of hydrophobic residues including the 6 Trp (*20*). In human c-Myb(R_2R_3) (*19*), the same as studied here, and B-Myb(R_2R_3) (*21*, *22*), only R_3 presents a similar structural organization with 3 Trp in the hydrophobic cluster whereas R_2 is flexible, especially so in the C-terminal part, thus exposing 3 Trp to the solvent. For these proteins, internal fluctuations can contribute to make all of the six Trp accessible.

A recent investigation has reported fluorescence data for R_2R_3 of the oncogenic mutant v-Myb and for the isolated R_3 (*18*, *28*). Interestingly, the comparison of R_3 with the wild-type R_2R_3 (same amino acid sequence as studied here) indicates that the three Trp in R_3 are on average less exposed than the six Trp in R_2R_3. In contrast, in the mutated v-Myb R_2R_3 (three point mutations occur in R_2 of v-Myb relative to c-Myb), the average exposure of the six Trp residues as deduced from acrylamide quenching is reduced with respect to the wild-type R_2R_3. Altogether, these data indicate that only a few sequence point mutations in R_2 can have a measurable influence on the dynamic properties of the minimal binding domain as a whole. This observation throws new light on the results of previous NMR investigations showing that the C-terminal part of R_2 can adopt a helical structure in mouse c-Myb (*17*) whereas it is characterized by conformational exchange in human, and chicken c-Myb and B-Myb (*19*, *21*, *22*).

Several changes occur when R_2R_3 binds DNA. They concern the structural environment and the dynamical accessibility of the Trp residues in the DNA-bound state. When the specific 1:1 (R_2R_3)−DNA complex is being formed (*23*), the maximum intensity of the fluorescence emission spectrum of Trp in R_2R_3 is shifted toward shorter wavelengths with respect to the free R_2R_3 domain. According to Burstein's spectral rules (*39*), this blue shift indicates that the overall fluorescence of R_2R_3 in the complex arises from Trp residues located in a more hydrophobic environment compared to the free R_2R_3; this means that on average the Trp side chains are less exposed to the aqueous solvent than in the free R_2R_3. In fact, shielding from the solvent is expected to occur more particularly for those side chains at the protein−DNA contact area directly involved in the specific interactions with the nucleotides in DNA. The large quenching of Trp fluorescence by DNA titration is consistent with the above observations and shows again that a profound modification of the fluorophore environment takes place. In fact, in the 1:1 (R_2R_3)−DNA specific complex four out of the six Trp residues are no longer solvent accessible, indicating that they belong to the contact region between the protein and DNA.

Two main mechanisms have been proposed to describe the quenching by nucleic acids of Trp emission in proteins: (i) a static quenching induced by stacking of the indole ring of the Trp residue with a purine or a pyrimidine ring (*40*−*42*); and (ii) a static or dynamic quenching due to a protein conformational change. The latter could be due to changes of the local environment of Trp induced by the binding to the oligonucleotide. These changes lead to a modification in the characteristics of the Trp fluorescence emission (*41*−*43*).

A previous NMR study provided the geometry of the mouse c-Myb(R_2R_3)−DNA complex (*17*). The side chains of Trp-95 and Trp-115 in R_2 and those of Trp-147 and Trp-166 in R_3 were found to have medium-range contacts (∼5 Å) either with the phosphate backbone of DNA or with protons of the ribose ring. Thus, despite the considerable difference between the experimental conditions between NMR and fluorescence (i.e., concentrations differing by 3−4 orders of magnitude), similar conclusions are reached as to the number of Trp residues involved in the R_2R_3−DNA interactions. This may be somehow surprising since, at the high protein−DNA concentration used for NMR (10^3 higher than the unspecific $K_d = 2.7 \times 10^{-6}$ M), unspecific complexes are expected to be predominant with the consequent presence of multiple protein DNA contacts (see Results). Perhaps c-Myb-DNA interface (specific and nonspecific) is always built with 4 Trp; however, the particular

Trp residues involved in the association surface would differ from one complex to another.

The absence of iodide quenching in the specific 1:1 complex is an additional monitor of the structural reorganization that occurs in R_2R_3 by DNA binding. A simple explanation for the absence of quenching might be that the Trp/iodide collisions are prevented by the negatively charged (R_2R_3)−DNA complex molecule. However, this effect alone cannot account by itself for the observed blue shift of the Trp fluorescence in the DNA-bound state (Figure 1).

For it to be compatible with the blue shift, the lack of iodide quenching must arise from a new structural organization of side chains surrounding the Trp residues in the complex; this reorganization would lead to a modification of the charge and the hydrophobic environment of the tryptophans. Thus, positively charged side-chains (e.g., Lys, Arg) close to Trp can establish ionic interactions with DNA, and this contributes both toward eliminating a possible interaction with iodide and toward increasing the local hydrophobicity. Alternatively, the side chain rearrangement could lead to the presence of negatively charged groups (Glu, Asp) in a new Trp environment. Consequently this can render inaccessible to iodide collisions the two exposed Trp residues that do not participate in direct contacts with the DNA.

The binding to DNA does not alter the number of accessible tryptophans to acrylamide in R_2R_3, indicating that the structural change does not modify the accessibility of the Trp fluorophores for this quencher. A slight but measurable and significant decrease of the Trp−acrylamide collisional rate constant k_q does, however, take place on going from the free to the bound R_2R_3 fragment (3×10^9 to 2.5×10^9 M^{-1} s^{-1}): it is worth noticing, though, that these values are 1 order of magnitude higher than the rate constant of the acrylamide−Trp collisions typically found in globular proteins (of the order of 2×10^8 M^{-1} s^{-1} (*36*)). These values represent the average dynamic behavior of the six tryptophans in the complex, in which four of them are closer to DNA and the two remaining are differently exposed to the solvent. Nonetheless, these findings imply that, in the bound state too, the R_2R_3 molecule presents a sufficiently high mobility to make the indole groups of all of the Trp residues accessible to acrylamide and to yield a collisional rate constant that, on average, is of the same order of magnitude as that observed for Trp in a random coil peptide (4×10^9 M^{-1} s^{-1}) (*38*).

The specific 1:1 (R_2R_3)−DNA complex found at low protein and DNA concentrations ($\approx 10^{-7}$ M) has a high affinity with a K_d value of 5×10^{-9} M (*23*); the formation of the specific complex is obtained (Figure 6) with two-step kinetics, with different rate constants. The first step observed after mixing of c-Myb(R_2R_3) with DNA_{mim16}, characterized by a fast bimolecular reaction rate constant ($k = 7 \times 10^5$ M^{-1} s^{-1}), should correspond to the Myb−DNA recognition and binding process; indeed, for most proteins, the association to small molecules is known to be a fast process (*37*, *44*−*46*). The second step of the complex formation is a slow first-order kinetic reaction ($k = 0.004$ s^{-1}). This part of the R_2R_3−DNA complex formation is likely to correspond to the change in the Trp environment associated to the structural reorganization of the side chains and to the redistribution of water molecules at the protein−DNA interface (*47*). Water molecules, mediating the protein−DNA contacts, are believed to play a crucial role in the recognition specificity and binding (*47*, *48*). Indeed protein atoms involved in binding to DNA occupy positions normally occupied by water molecules in unbound DNA (*49*). Moreover, these hydration sites represent the most probable and the energetically most favorable binding positions for hydrophilic DNA binders (*50*). Thus, the displacement of water molecules could contribute to increase the hydrophobicity of the Trp side chain environment, and partly account for the Trp fluorescence blue shift observed. Moreover water expulsion on the cMyb−DNA contacts cannot be accomplished without a higher viscosity of this interface. This could explain the slower rate of the second step.

Different lines of evidence have shown that, upon complex formation, and more specifically in dilute aqueous solution (as in this work), some bound water molecules located at the contact region between the protein and DNA (*47*, *48*) may be displaced to the continuum, thus making the protein−DNA interface more hydrophobic. Several examples indicate that, besides the reorganization of water, local conformational changes may occur upon DNA binding (*47*), more specifically in those cases where the protein is partly disordered in the absence of DNA: we report here evidence for this structural reorganization of side chains in the spatial proximity around the Trp fluorophores upon binding of Myb(R_2R_3) to DNA. This result is at variance with previous NMR work on mouse c-Myb(R_2R_3), indicating that no structural change occurs upon DNA binding (20). However, it is in agreement with the NMR observation of different DNA-bound forms of the same c-Myb(R_2R_3) sequence studied in this work. So, both the kinetic data and the increased hydrophobicity of the environment of the Trp are best explained as the result of the redistribution of water molecules and a protein conformational change. These alterations also provide strong arguments in favor of protein dynamics changes produced by the DNA−R_2R_3 association.

In conclusion, from this and other studies, differences in the conformational, dynamic, and thermodynamic behaviors are emerging for various R_2R_3 sequences of c-Myb and B-Myb, thus showing that point mutations in the N-terminal half of R_2 can have a major influence on either property (factor) and that these themselves bear consequences on DNA recognition.

REFERENCES

1. Shen-Ong, G. L. C. (1990) *Biochim. Biophys. Acta 1032*, 39−52.
2. Lüscher, B., and Eisenman, R. N. (1990) *Genes Dev. 4*, 2235−2241.
3. Introna, M., Luchetti, M., Castellano, M., Arsura, M., and Golay, J. (1994) *Cancer Biol. 5*, 113−124.
4. Ness, S. A., Marknell, A., and Graf, T. (1989) *Cell 59*, 1115−1125.
5. Evans, J. L., Moore, T. L., Kuehl, W. M., Bender, T., and Ting, J. P. (1990) *Mol. Cell. Biol. 10*, 5747−5752.
6. Zobel, A., Kalkbrenner, F., Guehmann, S., Nawrath, M., Vorbrueggen, G., and Moelling, K. (1991) *Oncogene 6*, 1397−1407.
7. Siu, G., Wurster, A. L., Lipsick, J. S., and Hedrick, S. M. (1992) *Mol. Cell. Biol. 12*, 1592−1604.
8. Sureau, A., Soret, J., Vellard, M., Crochet, J., and Perbal, B. (1992) *Proc. Natl. Acad. Sci. U.S.A. 89*, 11683−11687.
9. Biedenkapp, H., Borgmeyer, U., Sippel, A. E., and Klempnauer, K.-H. (1988) *Nature 335*, 835−837.

10. Weston, K., and Bishop, M. J. (1989) *Cell 58*, 85−93.
11. Ording, E., Kvavik, W., Bostad, A., and Gabrielsen O. S. (1994) *Eur. J. Biochem. 222*, 113−120.
12. Frampton, J., Gibson, T. J., Ness, S. A., Doderlein, G., and Graf, T. (1991) *Protein Eng. 4*, 891−901.
13. Anton, I. A., and Frampton, J. (1988) *Nature 336*, 719.
14. Frampton, J., Leutz, A., Gibson, T. J., and Graf, T. (1989) *Nature 342*, 134.
15. Sakura, H., Kanei-Ishii, C., Nagase, T., Nakagoshi, H., Gonda, T. J., and Ishii, S. (1989) *Proc. Natl. Acad. Sci. U.S.A. 86*, 5758−5762.
16. Howe, K. M., Reakes, C. F. L., and Watson, R. J. (1990) *EMBO J. 9*, 161−169.
17. Ogata, K., Morikawa, S., Nakamura, H., Sekikawa, A., Inoue, T., Kanai, H., Sarai, A., Ishii, S., and Nishimura, Y. (1994) *Cell 79*, 639−648.
18. Gabrielsen, O. S., Sentenac, A., and Fromageot, P. (1991) *Science 253*, 1140−1143.
19. Jamin, N., Gabrielsen, O. S., Gilles, N., Lirsac, P.-N., and Toma, F. (1993) *Eur. J. Biochem. 216*, 147−154.
20. Ogata, K., Morikawa, S., Nakamura, H., Hojo, H., Yoshimura, S., Zhang, R., Aimoto, S., Ametani, Y., Hirata, Z., Sarai, A., Ishii, S., and Nishimura, Y. (1995) *Nat. Struct. Biol. 2*, 309−320.
21. Carr, M. D., Wollborn, U., McIntosh, P. B., Frenkiel, T. A., McCormick, J. E., Bauer, C. J., Klempnauer, K −H., and Feeney, J. (1996) *Eur. J. Biochem. 235*, 721−735.
22. McIntosh, P. B., Frenkiel, T. A., Wollborn, U., McCormick, J. E., Klempnauer, K. H., Feeney, J., and Carr, M. D. (1998) *Biochemistry 37*, 9619−9629.
23. Jamin, N., Le Tilly, V., Zargarian, L., Bostad, A., Besançon-Yoshpe, I., Lirsac, P.-N., Gabrielsen, O. S., and Toma, F. (1996) *Int. J. Quantum Chem. 59*, 333−341.
24. Myrset, A. H., Bostad, A., Jamin, N., Lirsac, P.-N., Toma, F., and Gabrielsen, O. S. (1993) *EMBO J. 12*, 4625−4633.
25. Ebneth, A., Schweers, O., Thole, H., Fagin, U., Urbanke, C., Maass, G., and Wolfes, H. (1994) *Biochemistry 33*, 14586−14593.
26. Madan, A., Radha, P. K., Hosur, R. V., and Padhy, L. C. (1995) *Eur. J. Biochem. 232*, 150−158.
27. Madan, A., Radha, P. K., Srivastava, A., Padhy, L. C., and Hosur, R. V. (1995) *Eur. J. Biochem. 230*, 733−740.
28. Brendeford, E. M., Myrset, A. H., Hegvold, A. B., Lundlin, M., and Gabrielsen, O. S. (1997) *J. Biol. Chem. 272*, 4436−4443.
29. Fasman, G. D. (1979) in *Handbook of Biochemistry and Molecular Biology: Nucleic Acids*, 3rd ed., Vol. 1, p 589, CRC Press, Cleveland, OH.
30. Guehmann, S., Vorbrueggen, G., Kalkbrenner, F., and Moelling, K. (1992) *Nucleic Acids Res. 20*, 2279−2286.
31. Lakowicz, J. R., and Weber, G. (1973) *Biochemistry 12*, 21, 4171−4179.
32. Eftink, M. R., and Ghiron, C. A. (1976) *J. Phys. Chem. 80*, 486−493.
33. Lehrer, S. S. (1971) *Biochemistry 10*, 3254−3263.
34. Stern, O., and Volmer, M. (1919) *Phys. Z. 20*, 183−193.
35. Livesey, A. K., and Brochon, J. C. (1987) *Biophys. J. 52*, 693−706.
36. Eftink, M. R., and Ghiron, C. (1981) *Anal. Biochem. 114*, 199−227.
37. Pecht, I. (1982) in *The Antigenes* (Sela, Ed.) vol. VI, pp 1−62, New York.
38. Eftink, M. R., and Ghiron, C. A. (1976) *Biochemistry 15*, 3, 672−680.
39. Burstein, E. A., Vedenkina, N. S., and Ivkova, M. N. (1973) *Photochem. Photobiol. 18*, 263−279.
40. Mutai, K., Gruber, V. A., and Leonard, N. J. (1975) *J. Am. Chem. Soc. 97*, 4095−4104.
41. Hélène, C. (1977) *FEBS Lett. 74*, 10−13.
42. Hélène, C. (1977) in *Excited States in Organic Chemistry and Biochemistry* (Pullman, B., and Goldblum, N., Eds) pp 65−78, Reidel, Dordrecht, The Netherlands.
43. Maurizot, J. C., Boubault, G., and Hélène, C. (1978) *Biochemistry 17*, 2096−2101.
44. Fersht, A. (1985) in *Enzyme Structure and Mechanism* (Freeman, Ed.) 2nd ed., pp 147−153, New York.
45. Chaffotte, A., and Goldberg, M. E. (1987) *J. Mol. Biol. 197*, 131−140.
46. Friguet, B., Djavadi-Ohaniance, L., and Goldbeg, M. E. (1989) *Res. Immunol. 140*, 355−376.
47. Rhodes, D., Schwabe, J. W. R., Chapman, L., and Fairall, L. (1996) *Philos. Trans. R. Soc. London, Ser. B*, 501−509.
48. Schwabe, J. W. R. (1997) *Curr. Opin. Struct. Biol. 7*, 126−134.
49. Seeman, N. C., Rosenberg, J. M., and Rich, A. (1976) *Proc. Natl. Acad. Sci. U.S.A. 73*, 804−808.
50. Woda, J., Schneider, B., Patel, K., Mistry, K., and Berman, H. M. (1998) *Biophys. J. 75*, 2170−2177

BI981199J